Mixed-Solvent Engineering as a Way around the Trade-Off between Yield and Purity of (7,3) Single-Walled Carbon Nanotubes Obtained Using Conjugated Polymer Extraction

Dzienia, Andrzej

Just, Dominik

Taborowska, Patrycja

Mielanczyk, Anna

他

出版情報：Small. 19 (46), 2023-07-19. Wiley
バージョン：

NANO · MICRO small
www.small-journal.com

Mixed-Solvent Engineering as a Way around the Trade-Off between Yield and Purity of (7,3) Single-Walled Carbon Nanotubes Obtained Using Conjugated Polymer Extraction

Andrzej Dzienia, Dominik Just, Patrycja Taborowska, Anna Mielanczyk, Karolina Z. Milowska, Shunji Yorozuya, Sadahito Naka, Tomohiro Shiraki, and Dawid Janas**

The inability to purify nanomaterials such as single-walled carbon nanotubes (SWCNTs) to the desired extent hampers the progress in nanoscience. Various SWCNT types can be purified by extraction, but it is challenging to establish conditions giving rise to the isolation of high-purity fractions. The problem stems from the fact that common organic solvents or water cannot provide an optimal environment for purification. Consequently, one must often decide between the separation yield and purity of the product. This article reports how through the self-synthesis of poly(9,9-dioctylfluorene-alt-benzothiadiazole) with tailored characteristics, in-depth elucidation of the extraction process, and mixed-solvent engineering, a high-yield isolation of monochiral (7,3) SWCNTs is developed. The combination of toluene and tetralin affords a separation medium of unique properties, wherein both high yield and exceptional purity can be attained simultaneously. The reported results pave the way for further research on this rare chirality, which, as illustrated herein, is much more reactive than any of the previously separated SWCNTs.

1. Introduction

After many years of laborious and costly investigations, single-walled carbon nanotubes (SWCNTs) are finally on the verge of practical application. Owing to their unique features, they are applicable in the fields of electronics (nanocircuits,[1] field-effect transistors,[2,3] photonics (quantum computing, cryptography, and telecommunication,[4] and medicine (optical sensors for diagnostics,[5] among others. Beyond a doubt, these opportunities would not materialize without developing an arsenal of SWCNT sorting techniques.[6] Breakthroughs in this area have provided a critical mass of semiconducting SWCNTs (s-SWCNTs) for initial validation of their utility, which reignited the scientific community's interest in this nanomaterial.

Currently, s-SWCNTs can be harvested from unsorted SWCNT mixtures both in aqueous and organic media. In the former, SWCNTs are commonly differentiated by chromatography,[7] ultracentrifugation,[8] or aqueous two-phase extraction (ATPE).[9] In the latter, the most popular method involves wrapping SWCNTs with conjugated polymers (conjugated polymer extraction – CPE), which exhibit affinity toward species with specific chiral angles or diameters.[10,11] This is a very convenient approach as it

A. Dzienia, D. Just, P. Taborowska, A. Mielanczyk, D. Janas
Department of Chemistry
Silesian University of Technology
B. Krzywoustego 4, Gliwice 44-100, Poland
E-mail: andrzej.dzienia@polsl.pl; dawid.janas@polsl.pl

A. Dzienia
Institute of Materials Engineering
University of Silesia in Katowice
Bankowa 12, Katowice 40-007, Poland

K. Z. Milowska
CIC nanoGUNE
Donostia-San Sebastián 20018, Spain

K. Z. Milowska
Ikerbasque
Basque Foundation for Science
Bilbao 48013, Spain

K. Z. Milowska
TCM Group
Cavendish Laboratory
University of Cambridge
Cambridge CB3 0HE, UK

S. Yorozuya, S. Naka, T. Shiraki
Department of Applied Chemistry
Graduate School of Engineering
Kyushu University
744 Motooka, Nishi-ku, Fukuoka 819-0395, Japan

The ORCID identification number(s) for the author(s) of this article can be found under https://doi.org/10.1002/smll.202304211

DOI: 10.1002/smll.202304211

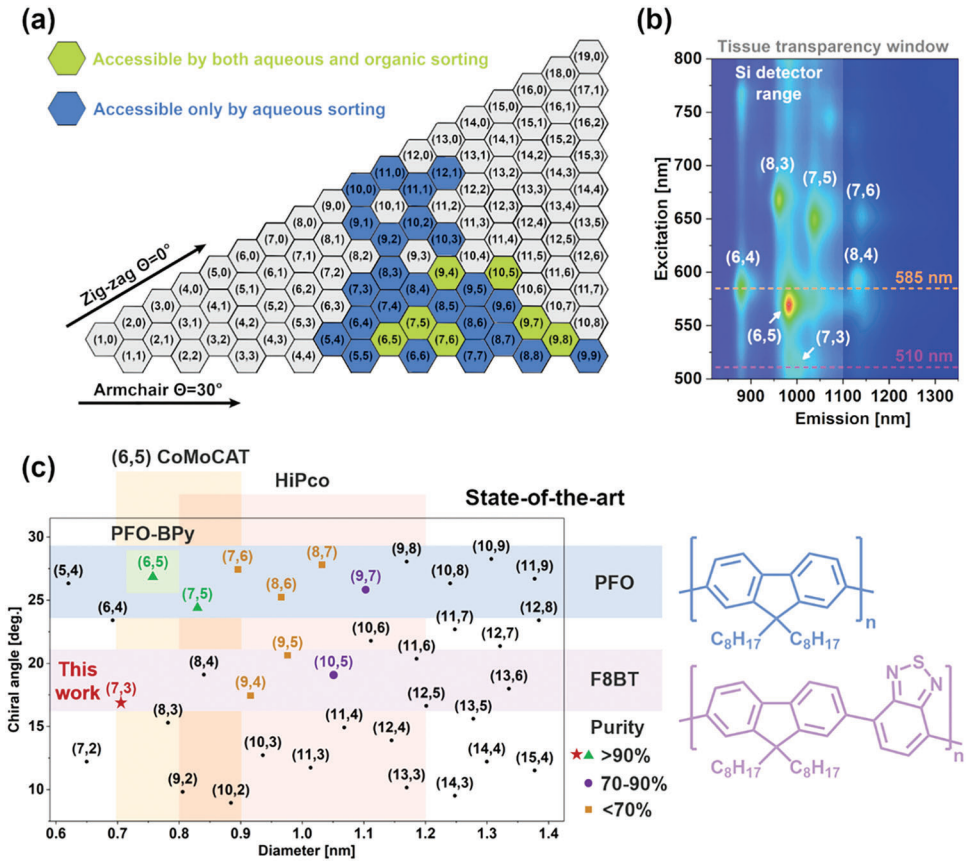

Figure 1. a) Chirality-enriched SWCNT fractions of various purity obtained in aqueous and non-aqueous media based on the literature data,[7,26,31–33] b) application opportunities of SWCNTs for theranostics using affordable Si detectors exemplified using photoluminescence (PL) excitation-emission map of (6,5)-enriched CoMoCAT SWCNTs dispersed in water with sodium deoxycholate (DOC), c) compilation of known selective methods for the isolation of SWCNTs from CoMoCAT and high-pressure carbon monoxide (HiPco) materials using polyfluorene derivatives. The purity was estimated using absorbance data provided in the literature.

produces suspensions of several SWCNT types, which can be directly deposited on many substrates due to the high volatility of typically employed organic solvents. Moreover, in many cases, CPE is considered the gold standard due to its far greater metallic nanotube removal efficiency,[12,13] better film-forming properties of organic dispersions,[14] and higher performance of the resulting nanocircuits.[15,16] Unfortunately, such an approach currently provides a much smaller selection of isolable monochiral SWCNTs compared with the differentiation of SWCNTs in aqueous media (**Figure 1**a).

The shortage of known effective methods for obtaining monochiral SWCNTs by CPE may be justified by the fact that the isolation, regardless of its easy execution nature, is a very complex issue in which only the appropriate simultaneous selection of several essential parameters leads to success. Scientists, through numerous experiments, identified combinations under which it is possible to increase the content of certain SWCNT species, such as (6,5), (7,5), (7,6), (8,6), (8,7), (9,4), (9,5), (9,8), (10,5), (10,6), (10,8), (12,5), and (15,4).[14,17–22] However, only the isolation of (6,5) and (7,5) provides truly monochiral material.

This paper reports a straightforward procedure for the synthesis and purification of polymers indispensable for CPE, such as poly(9,9-dioctylfluorene-2,7-diyl) (PFO), poly[(9,9-dioctylfluorenyl-2,7-diyl)-*alt*-co-(6,6′-{2,2′-bipyridine})] (PFO-BPy), and poly(9,9-dioctylfluorene-*alt*-benzothiadiazole) (F8BT) to make monochiral SWCNT species more abundant. The so-obtained polymers were used extensively to investigate the process of SWCNT differentiation in organic solvents. As a result, having interpreted the influence of key separation parameters, (7,3) SWCNTs of unprecedented purity were collected. Achieving the high quality of dispersion was possible due to the combination of in-house synthesized F8BT of suitable characteristics with a proper extraction medium. The application of higher-viscosity tetralin (rather than typically utilized toluene) substantially increased the concentration of suspended small-diameter SWCNTs such as (7,3) and (6,4). When a synergistic mixture of toluene and tetralin was used, monochiral (7,3) SWCNT fractions were produced with higher yields because of the optimized system composition and process parameters. To confirm the high utility of the obtained material, harvested SWCNTs were subjected to chemical

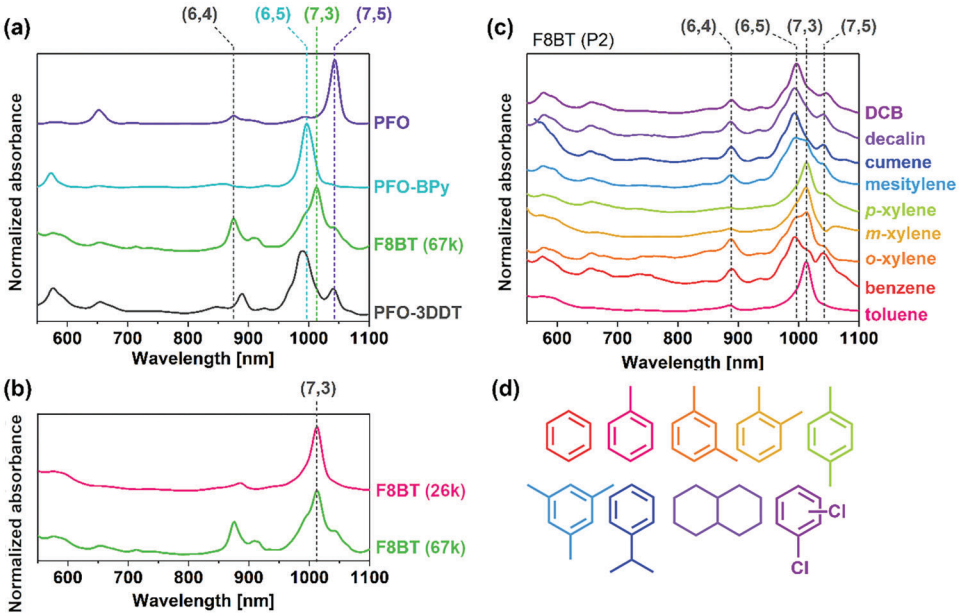

Figure 2. Normalized absorbance spectra of (6,5)-enriched CoMoCAT SWCNTs extracted with a) PFO, PFO-BPy, F8BT (M_n = 67k), PFO-3DDT (poly[(9,9-dioctylfluorenyl-2,7-diyl)-alt-(3-dodecylthiophene-2,5-diyl)]) in toluene, b) two F8BT batches (M_n = 26 and 67k) synthesized in-house using toluene as a solvent for extraction, c) F8BT (M_n = 26k) in various solvents. d) Chemical structures of the solvents employed.

functionalization in organic solvents to enhance their photonic properties.

2. Results and Discussion

Isolation of semiconducting SWCNTs with diameters <0.76 nm characteristic for (6,5) SWCNTs is demanding. So far, only (7,3), (6,4), and (5,4), have been harvested with reasonable purity while executing separation routines in aqueous conditions (Figure 1a).[23–26] Their emission not only fits within the optical transparency of human tissue but can also be detected by inexpensive silicon (Si) detectors (Figure 1b).

Unfortunately, processing SWCNTs in water may fill the SWCNT inner cavity with solvent molecules, thereby reducing the material's properties, such as carrier mobility.[27] One can find only a few studies on this matter since the diameters of these species are outside the diameter distribution reported for many commercially available raw materials, such as the popular HiPco[28,29] or other unsorted SWCNT materials. Thus, other materials with smaller SWCNT diameters, such as (6,5)-enriched CoMoCAT, can be employed to deal with this challenge. Nevertheless, there are no prior reports of extraction of SWCNTs other than (6,5) in the aforementioned low-diameter regime in organic solvents (Figure 1c). This issue limits the success of ongoing research to improve their photoluminescence quantum yield (PLQY) by chemical modification.[30] Such small-diameter SWCNTs should be more reactive due to their higher curvature, allowing them to broaden the scope of compatible chemical reactions.

2.1. Selection of Conjugated Polymer and Solvent

Our first trials to isolate SWCNTs in the small diameter regime from (6,5)-enriched CoMoCAT in toluene using F8BT (M_n = 67k) were only partially successful (**Figure 2**a). The absorbance spectrum indicated a polydisperse nature of the material and its absolute value was rather low. Nevertheless, closer investigation of the spectrum revealed the presence of a peak with a maximum of 1013 nm. Based on our previous experience isolating (6,5) using PFO-BPy shown in the plot, we concluded that F8BT would not likely cause such a strong redshift from 997 to 1013 nm.[34,35] Moreover, we did not detect a clear signal coming from the S_{22} transition of the (6,5) SWCNT, which typically occurs at 572 nm. Therefore, we deduced that our sorting parameters favor the enrichment of the material with (7,3) SWCNTs. According to the data reported for aqueous suspension, it has an S_{11} peak maximum between 992 and 1009 nm, while S_{22} is located between 494 and 510 nm. This assignment also explains the absence of a clear band from the S_{22} transition of (7,3) because it is masked by the absorbance from the polymer (Figure S6, Supporting Information).[22,28] However, by removing the polymer from the (7,3) SWCNT surface (Figure S7, Supporting Information), its fingerprint can be revealed.

Capitalizing on these promising results, we decided to verify if a different batch of F8BT, with lower molecular weight (M_n = 26k), would produce a more encouraging sorting outcome (Figure 2b). Indeed, dramatic improvement in terms of selectivity was observed. A nearly monochiral (7,3) fraction was produced, which confirmed the undeniable effect of the polymer nature on the separation course, which will be described in greater detail in the subsequent parts of the manuscript. Despite the successful outcome, we were not satisfied with the separation yield as the amount of extracted SWCNTs was insufficient, judging by the recorded absorbance values (Figure S8, Supporting Information).

For this reason, we tested whether the effectiveness of extraction can be enhanced using solvents with differences in

physicochemical properties (Figure 2c,d). In some reports, changing the nature of the solvent (e.g., density, viscosity, and dielectric constant) allows for tuning selectivity as well as suspension efficiency because the polymer and SWCNTs will behave differently in every medium.[17,20,36–41] Interestingly, even with small variations in the solvent properties (Table S1, Supporting Information) of benzene, toluene, *o*-, *m*-, and *p*-xylene, we noticed a substantial influence of the medium on the shape of the absorbance curves. Consequently, the concentration and the share of (7,3) suspended varied greatly. We conducted subsequent experiments with other solvents, such as mesitylene, cumene, decalin, or dichlorobenzene (DCB), but did not achieve the desired results. Regardless of differences in density, dipole moment, or viscosity, each time, the selectivity deviated from the optimal conditions established in toluene.

The addition of various alkyl moieties to the solvent's aromatic ring has a profound impact on the separation course. Note that aromatic toluene equipped with one methyl group offers appropriate solvent characteristics for the extraction, while extraction carried out in benzene solubilizes diverse SWCNT types. Similarly, *p*-xylene offers reasonable (7,3) SWCNT purity, supposedly due to the presence of alkyl moieties in favorable positions and its non-polar nature. The results demonstrate that CPE operates best in non-polar solvents, but the affinity toward specific SWCNTs is determined by the solvent nature. For instance, sorting in mesitylene was unsuccessful even though such a medium is aromatic, non-polar, and contains alkyl groups. Therefore, it is essential to establish a balance between the alkyl and aryl character of the separation medium to create a solvent with optimal characteristics for selective and effective SWCNT differentiation.

To validate our hypothesis that the proportion of alkyl and aryl parts is vital for establishing an appropriate environment for the separation, we engaged 1,2,3,4-tetrahydronaphthalene, commonly referred to as tetralin, for testing. Tetralin is a bicyclic molecule with distinct aromatic and aliphatic parts (**Figure 3**a,b). While the density and dielectric constant are slightly higher than those of toluene, the solvents differ very much in terms of viscosity and dipole moment. The former is nearly four times as high, whereas the latter is equal to zero, as tetralin does not have a dipole moment. An extension of the discussion related to the influence of the solvents' physicochemical parameters on CPE selectivity is available as supporting information (Section S9, Supporting Information).

The results of sorting in tetralin based on polymers with M_n = 26k, 65k (Ossila), and 67k (high M_w and dispersity) showed appreciable absolute absorbance values and selectivity toward (7,3) (Figure 3c; Figure S9, Supporting Information). Once again, the best outcome was obtained for F8BT (M_n = 26k). The only shortcoming is the noticeable presence of (6,4) SWCNTs, which have a similar diameter: 0.692 nm (6,4) versus 0.706 nm (7,3), but a different chiral angle, i.e., 23° versus 17°, respectively.

2.2. Partitioning Using SC SWCNT Dispersion and SC/TX100 Surfactant Mixture

Next, we aimed to optimize the mixture composition using the M_n = 26k polymer. We focused on the ratio of polymer to SWCNT in tetralin, as shown in **Figure 4**. One can observe a clear dependence of the spectrum shape on the ratio of polymer to SWCNT. At the two lowest excesses of a polymer by weight ratio to SWCNTs, i.e., 2:1 and 4:1, we observe a much lower suspension yield and an abundance of (6,5) SWCNTs in the supernatant. Then, the suspension efficiency, as well as the selectivity of (7,3) isolation versus other SWCNT species, increases as the polymer:SWCNT ratio is increased to 6:1. Further increasing the concentration of F8BT to the ratio of 7:1 contaminates the fraction with (6,4) SWCNTs, whereas the ratio 8:1 results in an excessive amount of polymer in the system. In such an environment, the concentration of free polymer chains is likely to remain consistently high even after some of the polymer molecules are bound to individualized SWCNTs. This, in turn, promotes the intensification of the aggregation processes of both the polymer chains and SWCNTs, causing both selectivity and suspension yield to decrease considerably. Based on this result, it appears that the optimal F8BT:SWCNT ratio is 6:1.

2.3. Mixed Solvent Engineering

Next, we tuned the behavior/microstructure of the polymer together with the properties of the above-discussed tetralin using the principles of an emerging approach called "mixed solvent engineering" to increase the resolution of the CPE system.[42] Mixed solvent engineering enables one to tailor the parameters of the medium for processing chemical compounds and materials by combining solvents of different properties. First, we tested the solvents used in the previous part of this work with tetralin at a 1:1 volume ratio. According to the absorbance spectra presented in Figure S10 (Supporting Information), the worst results were for the mixtures of tetralin with anisole and diphenyl ether, which show poor selectivity, as well as morpholine, which nullifies the effect of tetralin and results in a suspension composition close to the reference sample. In contrast, an interesting result is provided by the tetralin:THF sample, which shows good selectivity in the isolation of small-diameter SWCNTs such as (7,3) and (6,4). Lastly, excellent selectivity was obtained in the case of m-xylene, while the yield was quite low. In light of this promising result, we decided to test commonly employed toluene as a co-solvent.

When tetralin was combined with toluene, several benefits were achieved (**Figure 5**a). The first striking qualitative observation was that a 1:1 mixture of toluene and tetralin by volume produced a comparable selective isolation of (7,3) SWCNTs as when the process was conducted in pure toluene (even though the polarity, density, and dipole moment values were different).

On the other hand, when a 2:1 mixture of tetralin and toluene was employed, the shape of the spectra very much resembled that of the products of separation carried out in tetralin. The second discovery was that the combination of these two solvents provides a trade-off between selectivity and yield (Figure 5b). The fraction collected in tetralin:toluene (1:1) had a much-elevated concentration of (7,3) SWCNTs, while simultaneously the presence of (6,4) SWCNTs was minimized. Thus, by mixing toluene and tetralin, it is possible to obtain highly pure (7,3) SWCNTs in large quantities.

Most importantly, the characterization of the collected SWCNTs by PL excitation-emission mapping across a broad spectral range confirmed the exceptional purity of the produced

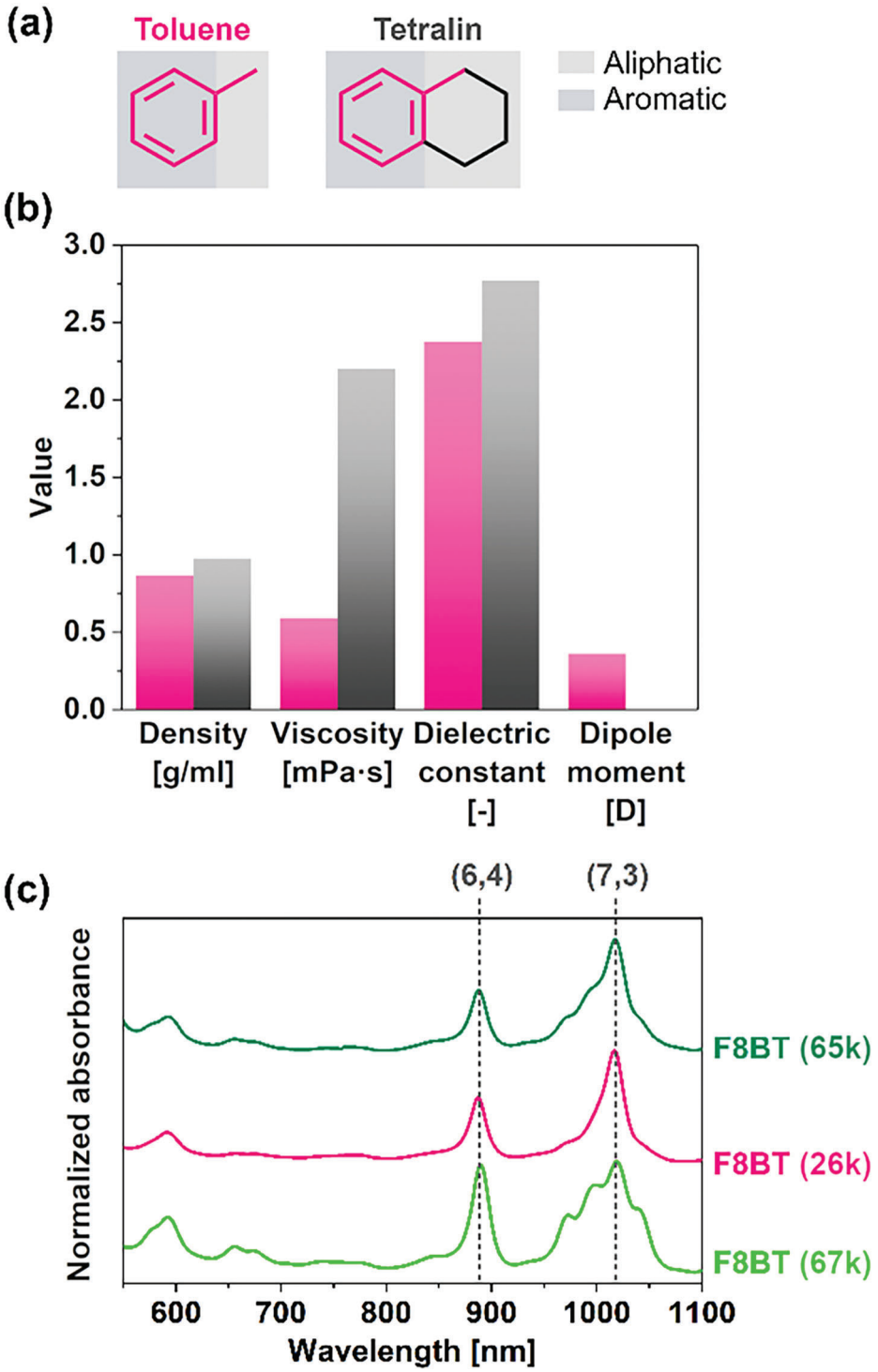

Figure 3. The difference in a) structure and b) selected properties of toluene and tetralin. c) Normalized absorbance spectra from SWCNT separation in tetralin using two previously discussed F8BT batches and a commercial (COM) F8BT reference obtained from the market.

fractions (Figure 5c,d). Regardless of the employed solvent, toluene (Figure 5c) or toluene:tetralin (1:1), only (7,3) SWCNTs were harvested from (6,5)-enriched CoMoCAT SWCNTs with F8BT using CPE. The amount of collected SWCNTs is relatively large as there was no need to remove F8BT for the analysis, the signal of which is present in the bottom left corner of the maps. Moreover, as expected, the PL analysis of the material suspended in tetralin confirmed that a polydisperse mixture of SWCNTs was obtained when only tetralin was employed (Figure S11, Supporting Information).

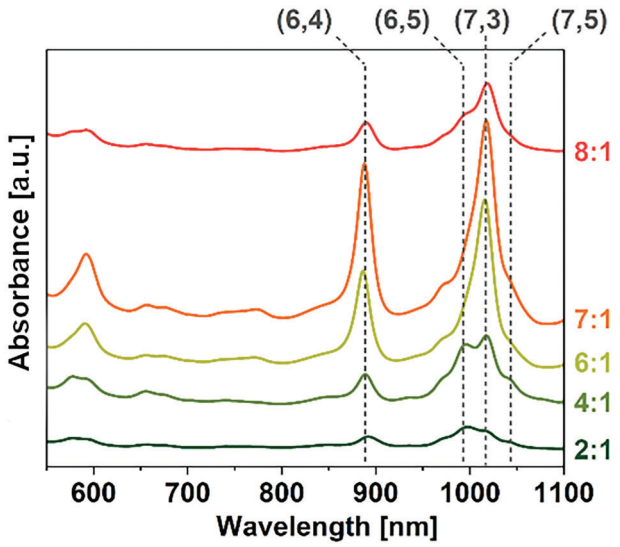

Figure 4. Absorbance spectra of SWCNTs isolated with different F8BT:SWCNT (M_n = 26k) ratios in tetralin.

Notably, the success of the CPE hinges upon a proper selection of raw materials for processing. While F8BT rendered excellent selectivity for (7,3) SWCNTs when (6,5)-enriched SWCNTs were suspended in toluene (Figure S12a, Supporting Information), inferior results were noted for the processing of (7,6)-enriched (Figure S12b, Supporting Information) and HiPco (Figure S12c, Supporting Information) SWCNTs. The other two material types did not enable chiral homogeneity to be reached. In both cases, (9,4) SWCNTs were the dominant type, accompanied by other species such as (6,4), (7,3), (7,5), (8,4), (8,7), or (9,2) SWCNTs. Therefore, one can conclude that there is a competitive affinity of (7,3) and (9,4) SWCNTs to F8BT, which agrees with the findings of Jakubka et al.[20] In the absence of the latter, it is possible to optimize the extraction conditions to reach monochiral purity. The successful outcome was validated with absorbance spectroscopy and cross-checked by PL excitation-emission mapping.

Concomitantly, the importance of the molecular weight of the selected F8BT should be recognized. In Figure 2b, we notice that appropriate characteristics of the polymer gave rise to promising separation outcomes in toluene. Therefore, we synthesized 6 batches of F8BT, used them for sorting (6,5)-enriched CoMoCAT SWCNTs (Figure S13, Supporting Information) in tetralin:toluene (1:1), and correlated the results with polymer characteristics determined by gel permeation chromatography (GPC) (Figure S14, Supporting Information). An optimal molecular weight of the polymer is required to effectively isolate (7,3) SWCNTs. The polymers with lower M_n (11 and 21k) were not as successful, possibly because of the insufficient length of the polymer chains. Conversely, higher M_n (44, 65, and 66k) polymers could not effectively wrap the targeted SWCNTs and promoted self-aggregation. F8BT, with a M_n of 26k, afforded the highest selectivity (both in toluene and toluene:tetralin), and seems optimal for sorting SWCNTs using this polymer under the selected conditions.

2.4. Evaluation of Enrichment Factor

After extensive work devoted to selective SWCNT harvesting was completed, it is worth quantifying how the performance and selectivity of SWCNTs changed during each stage. We used the PTF Fit[43] application to estimate the percentage of individual chiralities in the presented absorbance spectra (Table 1; Figure S15, Supporting Information). Although the accuracy of the fit may be susceptible to uncertainty using PTF Fit, this approach allows us to observe changes in the course of the suspension process that are necessary to decipher the correlations sorely missing in the literature between the type of polymer used, the solvents, the process conditions, and the final quality of the suspension.

The factor which is extremely important and often underestimated is the degree of enrichment, which demonstrates how selective a given polymer is under given conditions since this factor relates directly to the content of a given chirality in the starting material. This issue is worth emphasizing because it is much easier to selectively isolate a certain nanotube type from the pre-enriched starting material, e.g., increasing the percentage of (6,5) SWCNTs in CoMoCAT, which account for >50% (Table 1a), than analogous purification of other minor species. The results below show the composition of (6,5)-enriched SWCNTs from the CoMoCAT process. Many different types of SWCNTs can be discerned in the parent material, such as (6,5) (52.6%), (7,5) (14.5%), (8,3) (10.1%), (6,4) (10.1%), (7,3) (8.6%), etc.

The purification strategy reported herein reveals superb selectivity as *ca.* 90% pure (7,3) SWCNTs were harvested (Table 1b). The pristinity degree is on the order of *ca.* 90%, which matches that of (6,5) SWCNTs routinely collected using PFO-BPy and slightly exceeds that of (7,5) SWCNTs isolated with PFO (Table 1c,d). However, when one considers the concentration of these SWCNT types in the raw material, it becomes clear that remarkable enrichment is obtained using the strategy reported herein. While (7,5) and (6,5) SWCNTs are enriched by a factor of 3.72x (Table 1c) and 1.84x (Table 1d) using the aforementioned conjugated polymers (taking into account their abundance in the source material), our strategy enriches the material with (7,3) SWCNTs by a factor of 13.33x (Table 1b). In addition, this quantification procedure emphasizes that detailed analysis of the absorbance spectra is crucial because certain SWCNT species may not be identified using only PL. For example, the acquired PL excitation-emission maps suggested that only (6,5) and (7,5) SWCNTs are obtained by CPE using PFO-BPy (Figure S16a, Supporting Information) and PFO (Figure S16b, Supporting Information), respectively. At the same time, the optical absorbance data unquestionably revealed the presence of other SWCNT species, however minor their content may be.

2.5. Modeling of the SWCNT-Polymer-Solvent Interactions

We engaged molecular dynamics simulations and time-step Monte Carlo modeling to elucidate the underlying phenomena enabling extraordinary sorting of SWCNTs. We have modeled interactions between F8BT polymer and two different SWCNTs: (7,3) and (6,4), suspended in a toluene, tetralin, or a toluene-tetralin (equal number of molecules) mixture (Figure S17, Supporting Information). The simulation results

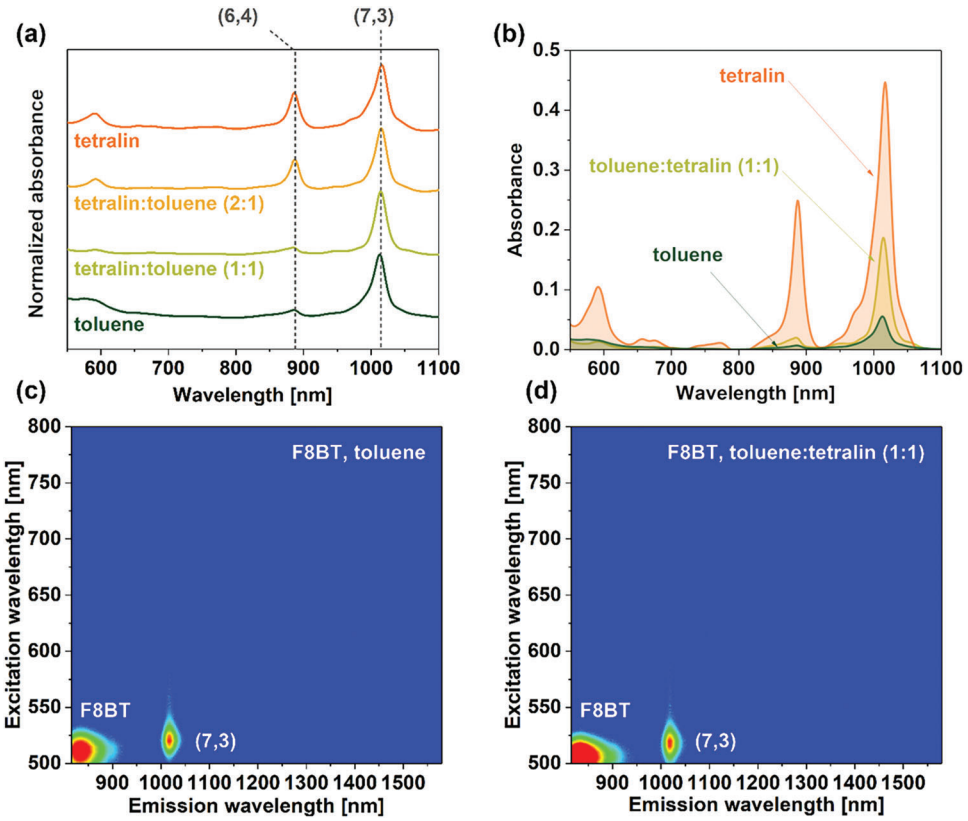

Figure 5. a) Normalized absorbance spectra of SWCNTs isolated with F8BT (M_n = 26k) in tetralin, tetralin:toluene (2:1), tetralin:toluene (1:1), and toluene, b) comparison of the absolute absorbance of SWCNT suspensions made by the application of F8BT in tetralin, toluene:tetralin (1:1), and toluene. PL excitation-emission maps of (7,3) SWCNT harvested in c) toluene and d) toluene:tetralin (1:1).

Table 1. Quantification of the individual SWCNT chirality percentages in the collected fractions using the indicated polymers and solvents determined by the PTF Fit application. The most abundant SWCNT types are highlighted.

SWCNT type	(a) PFO-3DDT in toluene	(b) F8BT (26k) in toluene:tetralin (1:1)	(c) PFO in toluene	(d) PFO-BPy in toluene
(7,3)	8.6	89.0	4.2	2.3
(6,4)	10.1	5.7	0.3	-
(7,5)	14.5	0.3	81.4	0.3
(9,1)	2.3	1.4	-	1.7
(6,5)	52.6	3.6	9.0	90.4
(8,3)	10.1	-	2.9	4.9
(5,4)	1.1	-	1.8	0.5
(8,1)	0.8	-	0.3	-
Enrichment factor	-	13.33x	3.72x	1.84x

presented in **Figure 6** indicate that the interactions between the SWCNT and the polymer depend on the nanotube chirality (Figure 6a,b) as well as the solvent (Figure 6b,c).

F8BT polymer has two distinct structural parts: the backbone and the side chains, which could be differently oriented to the nanotube lateral surface. As can be seen in Figure 6a, in the equal mixture of tetralin and toluene, F8BT preferentially orients the majority of its backbone next to the (7,3) nanotube. At the same time, in the case of (6,4) SWCNT, F8BT side chains are positioned closer to the nanotube than the F8BT backbone. This suggests stronger interaction between F8BT and (7,3) SWCNT than between F8BT and (6,4) SWCNT, laying the groundwork for effective selective isolation of the former. This is also reflected in the radial distribution function (RDF) analysis, which indicates that the probability of finding polymer next to (7,3) SWCNT is higher than in the case of (6,4) SWCNT (*cf.* magnitude of both RDFs presented in Figure 6b, medium left panel). It also shows that the minimal distance between the nanotube and polymer atoms

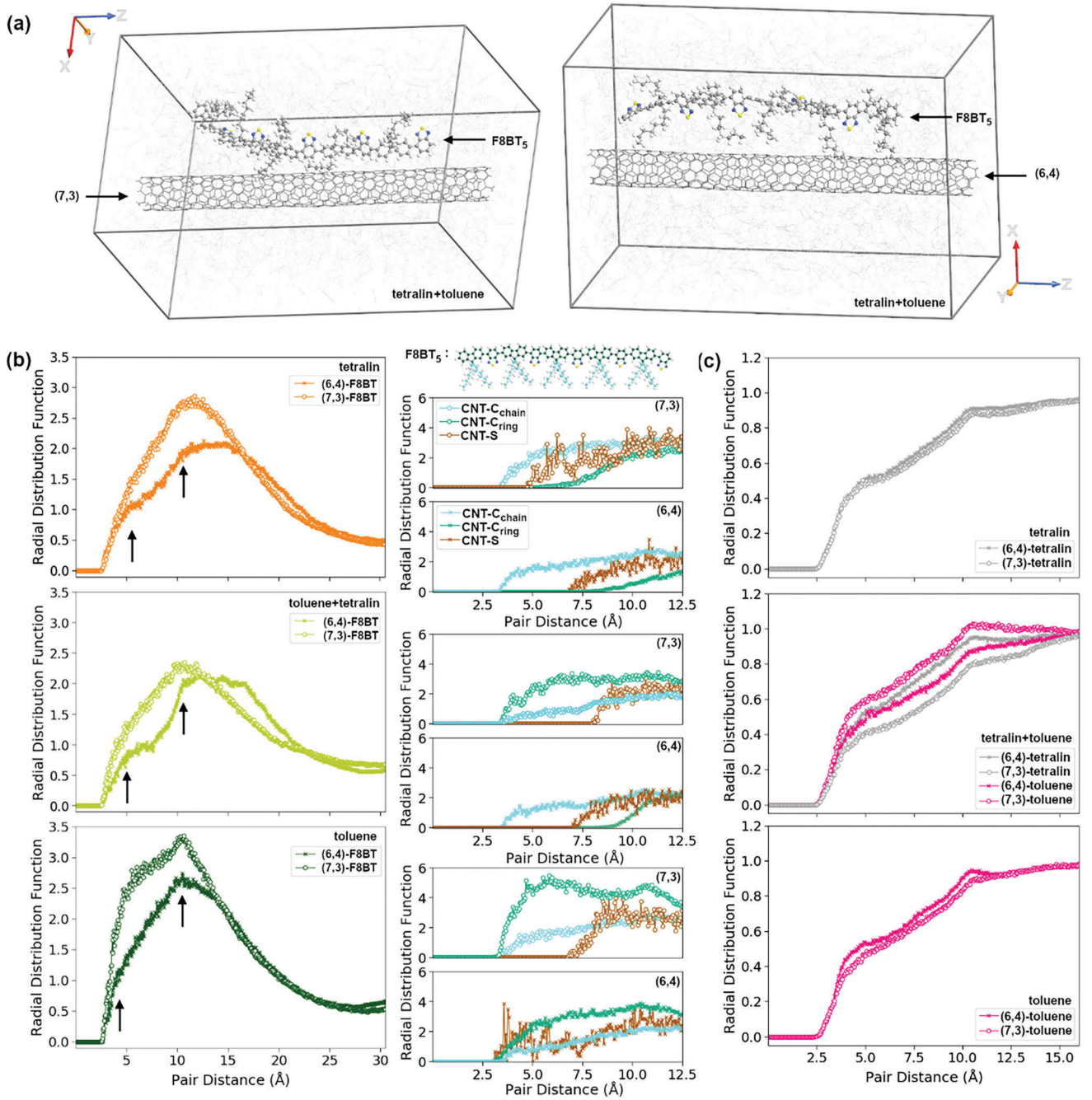

Figure 6. a) Snapshots of the final configuration for the simulation box containing (left) two units of (7,3) or (right) four units of (6,4) carbon nanotubes interacting with F8BT (five monomers) in toluene (350 molecules)-tetralin (350 molecules) solution. SWCNTs, solvent, and polymer molecules are represented using stick, line, and ball-and-stick models, respectively. For clarity, solvent molecules are drawn with a higher degree of transparency than other system components. C atoms are depicted in dark grey, while O, S, N, and H are shown in red, yellow, navy blue, and white, respectively. b) The impact of the solvent type on interactions between the polymer and different SWCNTs in ternary (SWCNT+polymer+solvent) systems. Left panel: Comparison of the radial distribution function (RDF) of nanotube-polymer atoms for systems containing (7,3) or (6,4) SWCNTs. Right panel: RDF between nanotube carbon and polymer backbone carbon (C_{ring}) atoms, nanotube carbon and polymer side chain (C_{chain}) atoms, nanotube carbon, and polymer sulfur atoms for both types of SWCNTs immersed in toluene (700 molecules), tetralin (700 molecules) or equal toluene-to-tetralin (350:350) solution. A schematic diagram showing two distinct regions of F8BT polymer: the backbone and the side chains is displayed above RDFs. All carbon atoms constituting polymer backbone are marked in teal, whereas carbon atoms forming side chains are cyan. c) Interactions between solvent molecules and different SWCNTs in ternary (SWCNT+polymer+solvent) systems. RDFs between nanotube carbon and solvent atoms.

is smaller for (7,3) SWCNT than for (6,4) CNTs (*cf*. positions of the first peaks in the RDFs presented in Figure 6b, medium left panel), which confirms "molecular matching" in (7,3)/F8BT nanocomposites. In contrast to the RDF between (7,3) SWCNT and polymer, the RDF between (6,4) SWCNT and polymer possesses two clearly separated peaks which indicates that two distinct parts of polymer are positioned at different distances from the (6,4) SWCNT. The more detailed RDF analysis (Figure 6b, medium right panel) confirms that F8BT side chains are positioned considerably closer to the (6,4) SWCNT than the F8BT backbone. The minimal distance between (6,4) SWCNT and polymer side chain atoms is smaller than 4 Å, while the minimal distance between (6,4) SWCNT and polymer backbone is larger than 10 Å. In the case of (7,3) SWCNT, the minimal distance between F8BT backbone and nanotube, only *ca*. 4. Å, is slightly smaller than the minimal distance between F8BT side chains and nanotube (*cf*. position of the first peak of (7,3)-C_{chain} and (7,3)-C_{ring} in Figure 6b, medium left panel).

Comparison between the first-to-second peak magnitude ratio of SWCNT-F8BT RDFs marked by arrows in Figure 6b (left panel) reveals the differences in SWCNT-F8BT interactions in different solvents. For example, changing the solvent from the toluene-tetralin mixture to only toluene (Figure 6b bottom left panel) moves F8BT away from (6,4) SWCNT (the ratio decreases with respect to the tetralin-toluene mixture) but brings F8BT closer to (7,3) SWCNT (the magnitude of the first (7,3)-F8BT RDF peak is similar to the magnitude of the second (7,3)-F8BT RDF peak). Therefore, the selectivity of F8BT toward (7,3) is improved in pure toluene, which follows the experimental results presented above. Moreover, if only toluene is present in the system, the differences in orientation of distinct polymer regions toward the nanotube lateral surface become smaller (Figure 6b, bottom right panel). The minimal distance between polymer side chains and the nanotube is similar to that between the polymer backbone and nanotube for both SWCNTs. Polymer side chains and backbones become preferentially positioned close to the (7,3) SWCNT, as well as to the (6,4) SWCNT. Although in the case of (6,4) SWCNT, one can observe the reduction of the minimal distance between the sulfur polymer backbone and nanotube atoms – from *ca*. 7.5 Å in the toluene-tetralin mixture to only *ca*. 3.5 Å in toluene. This indicates different orientations of the polymer backbones toward (7,3) and (6,4) SWCNTs.

On the other hand, using only tetralin as a solvent (Figure 6b, top right panel) produces significant differences in the interaction of distinct polymer regions with both nanotubes. The minimal distance between polymer side chains and nanotube is smaller (*ca*. 4 Å) than the minimal distance between the polymer backbone and nanotube (larger than 6 Å for (7,3) SWCNT and larger than 8 Å for (6,4) SWCNT). Moreover, the minimal distance between polymer sulfur and (7,3) SWCNT atoms becomes smaller when only tetralin is present, suggesting a change in the orientation of the polymer backbone toward this SWCNT with respect to its direction in the toluene-tetralin mixture. As RDF analysis reveals (Figure 6b, top left panel), F8BT is positioned closer to (6,4) SWCNT in tetralin than in the toluene-tetralin mixture (*cf*. F8BT-(6,4) RDFs in Figure 6b, top left and medium left panels). At the same time, F8BT moves slightly away from (7,3) SWCNT. However, note that the probability of finding F8BT next to (7,3) SWCNT is still much larger than the probability of detecting F8BT next to the (6,4) SWCNT, explaining why (7,3) SWCNTs were predominantly isolated from all three (toluene, toluene-tetralin, and tetralin) solutions. Nonetheless, the increased probability of finding an F8BT molecule next to (6,4) SWCNT explains why the relative content of (6,4) SWCNTs with respect to (7,3) SWCNTs increases after raw material sorting in pure tetralin (Figure 5a).

Interestingly, varying the type of solvent in the ternary systems also induces changes in the interactions between solvent molecules and different types of SWCNT. As can be seen in Figure 6c, the most significant differences between (6,4) and (7,3) SWCNT and their interaction with solvents are visible when nanotubes are placed in toluene-tetralin or toluene solutions. On the contrary, solvent-SWCNT RDFs are similar when both nanotubes are placed in tetralin. This observation, together with the previous analysis of interactions between F8BT polymer and SWCNTs, might explain why both nanotubes are harvested from tetralin using F8BT polymer, while the application of toluene-tetralin or pure toluene promotes exclusive isolation of (7,3) SWCNTs.

The additional MD/MC simulations also validated the findings reported in Figure S13 (Supporting Information) that the polymer length (Figure S18, Supporting Information) substantially impacts the interactions between polymer and nanotubes and thus affects the ability of the selective sorting of particular types of SWCNTs. F8BT of insufficient length (three monomers instead of five) offers markedly lower (7,3) selectivity in different solvents. This justifies our earlier observations that the short F8BT chains have an increased tendency to extract (6,4) SWCNTs with respect to the polymer of the optimal molecular weight (M_n = 26k). As confirmed by modeling in Figures S19 and S20 (Supporting Information), assembly of a tight F8BT coating on SWCNTs is essential for the polymer to offer selective sorting of SWCNTs, even in the case of chiralities that are very challenging to discriminate, such as (6,4) and (7,3). Ghosh et al. reported that the densities of these types of SWCNTs suspended by sodium cholate in water are almost indistinguishable.[44] While modeling, we calculated the diffusion coefficients of (6,4) and (7,3) SWCNTs wrapped with 14x$F8BT_5$ molecules in a mixture of tetralin and toluene (1400:1400). The coefficients were found to be $D_{(6,4)} = 8.58 \times 10^{-9} \pm 1.80 \times 10^{-11}$ cm^2 s^{-1} (R^2 = 0.990) and $D_{(7,3)} = 8.39 \times 10^{-9} \pm 1.46 \times 10^{-11}$ cm^2 s^{-1} (R^2 = 0.993), respectively. The negligible difference between the two explains why the collected (7,3) SWCNT fractions are commonly contaminated with (6,4) SWCNTs. Moreover, this also indicates a remarkable tunability of the CPE platform, which enabled us to obtain a monochiral (7,3) suspension. As the diffusion coefficients are very similar, this outcome could not have been achieved by simple ultracentrifugation,[14] which is a commonly employed method for enhancing SWCNT discrimination by CPE.

Finally, we subjected the material to chemical modification to demonstrate the notable practical utility of (7,3) SWCNTs obtained using the developed methodology (Figure S21, Supporting Information). Due to the high reactivity of small-diameter SWCNTs, easily obtainable (6,5) SWCNTs are a valuable asset in nanochemistry and nanophotonics. However, since other SWCNTs in the small-diameter regime are unavailable in large quantities, understanding how the chiral angle affects the SWCNT grafting mechanism remains limited. The emergence of the E_{11}^* defect peak[45] confirms that the surface of (7,3) SWCNTs can be

tailored straightforwardly, contrary to larger species such as (7,5) SWCNTs that show negligible reactivity under the same conditions. Importantly, introducing defects in the E_{11}^{*} binding configuration produced an optical trap depth as large as 143 meV. As this value can be further enhanced by creating E_{11}^{*-}-type defects on the (7,3) SWCNTs, the harvested material appears particularly promising for a broad spectrum of photonic applications.

3. Conclusion

Although many years of development have elapsed in SWCNT processing, simple methods for large-scale isolation of specific SWCNTs are still lacking, hindering progress in the field and consequently delaying the widespread use of SWCNTs. The multistep nature of the separation protocols, the lack of reproducibility, and the need for sophisticated apparatus are the main culprits of this problem. At the root of this lies the low availability and high price of the conjugated polymers utilized in the CPE process.

Taking this into account, we present a readily accessible method to synthesize CPE-relevant polymers with various macromolecular parameters. Solving this issue enables us to isolate small-diameter SWCNTs using conjugated polymers in organic solvents, which is necessary to further develop the field of photonics. The most significant achievement of the present work is the demonstration of a one-step method for the selective isolation of monochiral (7,3) SWCNTs. Additionally, we explain the entire optimization process with a focus on the key aspects responsible for the success of the sorting procedure. Notably, resignation from the application of ultracentrifugation in high overloads or density gradients significantly increases the potential scalability of the developed protocol. That is because the selectivity of the process in the devised approach is not enhanced at the expense of the extraction yield.

4. Experimental Section

All the information about the materials and methods is provided in the Supplementary Information.

Supporting Information

Supporting Information is available from the Wiley Online Library or from the author.

Acknowledgements

The authors would like to thank the National Science Centre, Poland (under the SONATA program, Grant agreement 2020/39/D/ST5/00285) for financial support of the research and the Polish National Agency for Academic Exchange for enabling and carrying out preliminary research abroad that laid the foundation for this study (BPI/PST/2021/1/00039).

Conflict of Interest

The authors declare no conflict of interest.

Data availability statement

The data that support the findings of this study are available from the corresponding author upon reasonable request.

Keywords

extraction, polymers, purification, single-walled carbon nanotubes

Received: May 19, 2023
Revised: July 11, 2023
Published online: July 19, 2023

[1] S. H. Chae, Y. H. Lee, *Nano Convergence* **2014**, *1*, 15.
[2] X. He, H. Htoon, S. K. Doorn, W. H. P. Pernice, F. Pyatkov, R. Krupke, A. Jeantet, Y. Chassagneux, C. Voisin, *Nat. Mater.* **2018**, *17*, 663.
[3] S. Forel, L. Sacco, A. Castan, I. Florea, C. S. Cojocaru, *Nanoscale Adv.* **2021**, *3*, 1582.
[4] A. Saha, B. J. Gifford, X. He, G. Ao, M. Zheng, H. Kataura, H. Htoon, S. Kilina, S. Tretiak, S. K. Doorn, *Nat. Chem.* **2018**, *10*, 1089.
[5] Z. Yaari, Y. Yang, E. Apfelbaum, C. Cupo, A. H. Settle, Q. Cullen, W. Cai, K. L. Roche, D. A. Levine, M. Fleisher, L. Ramanathan, M. Zheng, A. Jagota, D. A. Heller, *Sci. Adv.* **2021**, *7*, eabj0852.
[6] D. Janas, *Mater. Chem. Front.* **2018**, *2*, 36.
[7] D. Yang, L. Li, X. Wei, Y. Wang, W. Zhou, H. Kataura, S. Xie, H. Liu, *Sci. Adv.* **2021**, *7*, eabe0084.
[8] S. Cambré, W. Wenseleers, *Angew. Chem., Int. Ed.* **2011**, *50*, 2764.
[9] J. A. Fagan, *Nanoscale Adv.* **2019**, *1*, 3307.
[10] J. Wang, T. Lei, *Polymers* **2020**, *12*, 1548.
[11] F. Liu, X. Chen, M. Xi, N. Wei, L. Bai, L. Peng, Y. Cao, X. Liang, *Nano Res.* **2022**, *15*, 8479.
[12] S. K. Samanta, M. Fritsch, U. Scherf, W. Gomulya, S. Z. Bisri, M. A. Loi, *Acc. Chem. Res.* **2014**, *47*, 2446.
[13] T. Srimani, J. Ding, A. Yu, P. Kanhaiya, C. Lau, R. Ho, J. Humes, C. T. Kingston, P. R. L. Malenfant, M. M. Shulaker, *Adv. Electron. Mater.* **2022**, *8*, 2101377.
[14] Y. Li, M. Zheng, J. Yao, W. Gong, Y. Li, J. Tang, S. Feng, R. Han, Q. Sui, S. Qiu, L. Kang, H. Jin, D. Sun, Q. Li, *Adv. Funct. Mater.* **2022**, *32*, 2107119.
[15] L. Liu, J. Han, L. Xu, J. Zhou, C. Zhao, S. Ding, H. Shi, M. Xiao, L. Ding, Z. Ma, C. Jin, Z. Zhang, L.-M. Peng, *Science* **2020**, *368*, 850.
[16] G. Hills, C. Lau, A. Wright, S. Fuller, M. D. Bishop, T. Srimani, P. Kanhaiya, R. Ho, A. Amer, Y. Stein, D. Murphy, Arvind, A. C., M. M. Shulaker, *Nature* **2019**, *572*, 595.
[17] H. Ozawa, N. Ide, T. Fujigaya, Y. Niidome, N. Nakashima, *Chem. Lett.* **2011**, *40*, 239.
[18] A. Nish, J.-Y. Hwang, J. Doig, R. J. Nicholas, *Nat. Nanotechnol.* **2007**, *2*, 640.
[19] J. Ouyang, H. Shin, P. Finnie, J. Ding, C. Guo, Z. Li, Y. Chen, L. Wei, A. J. Wu, S. Moisa, F. Lapointe, P. R. L. Malenfant, *ACS Appl. Polym. Mater.* **2022**, *4*, 6239.
[20] F. Jakubka, S. P. Schießl, S. Martin, J. M. Englert, F. Hauke, A. Hirsch, J. Zaumseil, *ACS Macro Lett.* **2012**, *1*, 815.
[21] R. Si, L. Wei, H. Wang, D. Su, S. H. Mushrif, Y. Chen, *Chem. Asian J.* **2014**, *9*, 868.
[22] M. Tange, T. Okazaki, S. Iijima, *J. Am. Chem. Soc.* **2011**, *133*, 11908.
[23] E. Shimura, T. Tanaka, Y. Kuwahara, T. Saito, T. Sugai, S. Kuwahara, *RSC Adv.* **2020**, *10*, 24570.
[24] J. A. Fagan, C. Y. Khripin, C. A. Silvera Batista, J. R. Simpson, E. H. Hároz, A. R. Hight Walker, M. Zheng, *Adv. Mater.* **2014**, *26*, 2800.
[25] A. A. Green, M. C. Duch, M. C. Hersam, *Nano Res.* **2009**, *2*, 69.
[26] M. Kim, X. Wu, G. Ao, X. He, H. Kwon, N. F. Hartmann, M. Zheng, S. K. Doorn, Y. Wang, *Chem* **2018**, *4*, 2180.
[27] S. Chakraborty, H. Kumar, C. Dasgupta, P. K. Maiti, *Acc. Chem. Res.* **2017**, *50*, 2139.
[28] N. Berton, F. Lemasson, F. Hennrich, M. M. Kappes, M. Mayor, *Chem. Commun.* **2012**, *48*, 2516.

[29] B. Podlesny, T. Shiraki, D. Janas, *Sci. Rep.* **2020**, *10*, 9250.
[30] T. Shiraki, Y. Miyauchi, K. Matsuda, N. Nakashima, *Acc. Chem. Res.* **2020**, *53*, 1846.
[31] Y. Piao, B. Meany, L. R. Powell, N. Valley, H. Kwon, G. C. Schatz, Y. Wang, *Nat. Chem.* **2013**, *5*, 840.
[32] G. Ao, J. K. Streit, J. A. Fagan, M. Zheng, *J. Am. Chem. Soc.* **2016**, *138*, 16677.
[33] Z. Lin, Y. Yang, A. Jagota, M. Zheng, *ACS Nano* **2022**, *16*, 4705.
[34] K. S. Mistry, B. A. Larsen, J. L. Blackburn, *ACS Nano* **2013**, *7*, 2231.
[35] P. Zhang, W. Yi, L. Bai, Y. Tian, J. Hou, W. Jin, J. Si, X. Hou, *Chem. Asian J.* **2019**, *14*, 3855.
[36] H. Wang, B. Hsieh, G. Jiménez-Osés, P. Liu, C. J. Tassone, Y. Diao, T. Lei, K. N. Houk, Z. Bao, *Small* **2015**, *11*, 126.
[37] J. Ouyang, J. Ding, J. Lefebvre, Z. Li, C. Guo, A. J. Kell, P. R. L. Malenfant, *ACS Nano* **2018**, *12*, 1910.
[38] S. Qiu, K. Wu, B. Gao, L. Li, H. Jin, Q. Li, *Adv. Mater.* **2019**, *31*, 1800750.
[39] L. Qian, W. Xu, X. Fan, C. Wang, J. Zhang, J. Zhao, Z. Cui, *J. Phys. Chem. C* **2013**, *117*, 18243.
[40] H. Zhu, L. Hong, H. Tanaka, X. Ma, C. Yang, *Bull. Chem. Soc. Jpn.* **2021**, *94*, 1166.
[41] T. Shiraki, Y. Niidome, F. Toshimitsu, T. Shiraishi, T. Shiga, B. Yu, T. Fujigaya, *Chem. Commun.* **2019**, *55*, 3662.
[42] S. Cho, P. Pandey, J. Park, T.-W. Lee, D.-W. Kang, *ACS Appl. Energy Mater.* **2022**, *5*, 387.
[43] M. Pfohl, D. D. Tune, A. Graf, J. Zaumseil, R. Krupke, B. S. Flavel, *ACS Omega* **2017**, *2*, 1163.
[44] S. Ghosh, S. M. Bachilo, R. B. Weisman, *Nat. Nanotechnol.* **2010**, *5*, 443.
[45] D. Janas, *Mater. Horiz.* **2020**, *7*, 2860.